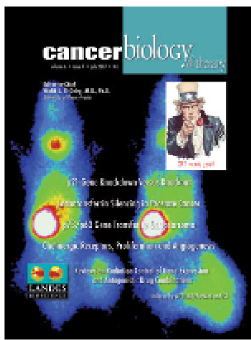

Taylor & Francis
Taylor & Francis Group

Cancer Biology & Therapy

ISSN: 1538-4047 (Print) 1555-8576 (Online) Journal homepage: http://www.tandfonline.com/loi/kcbt20

Furanodiene induces G2/M cell cycle arrest and apoptosis through MAPK signaling and mitochondria-caspase pathway in human hepatocellular carcinoma cells

Yu Xiao, Yang Feng-Qing, Li Shao-Ping, Gao Jian-Li, Hu Guang, Lao Sin-Cheng, Conceição Leong Emilia, Fung Kwok-Pui, Wang Yi-Tao & Lee Ming-Yuen Simon

To cite this article: Yu Xiao, Yang Feng-Qing, Li Shao-Ping, Gao Jian-Li, Hu Guang, Lao Sin-Cheng, Conceição Leong Emilia, Fung Kwok-Pui, Wang Yi-Tao & Lee Ming-Yuen Simon (2007) Furanodiene induces G2/M cell cycle arrest and apoptosis through MAPK signaling and mitochondria-caspase pathway in human hepatocellular carcinoma cells, Cancer Biology & Therapy, 6:7, 1044-1050, DOI: 10.4161/cbt.6.7.4317

To link to this article: https://doi.org/10.4161/cbt.6.7.4317

Published online: 11 Jul 2007.

Submit your article to this journal

Article views: 213

Citing articles: 41 View citing articles

Full Terms & Conditions of access and use can be found at
http://www.tandfonline.com/action/journalInformation?journalCode=kcbt20

[Cancer Biology & Therapy 6:7, 1044-1050; July 2007]; ©2007 Landes Bioscience

Research Paper

Furanodiene Induces G_2/M Cell Cycle Arrest and Apoptosis Through MAPK Signaling and Mitochondria-Caspase Pathway in Human Hepatocellular Carcinoma Cells

Yu Xiao[1,2]
Feng-Qing Yang[1]
Shao-Ping Li[1]
Jian-Li Gao[1]
Guang Hu[1]
Sin-Cheng Lao[1]
Emilia Leong Conceição[1]
Kwok-Pui Fung[3,4]
Yi-Tao Wang[1,*]
Simon Ming-Yuen Lee[1,4,*]

[1]Institute of Chinese Medical Sciences; University of Macau; Taipa, Macao, P.R. China

[2]State Drug Clinical Trial Agency; Science & Technology Department; Sichuan Provincial People's Hospital; Sichuan Academy of Medical Science; Chengdu, P.R. China

[3]Department of Biochemistry; [4]Institute of Chinese Medical; The Chinese University of Hong Kong; Hong Kong, China

*Correspondence to: Dr. Simon Ming Yuen Lee; Institute of Chinese Medical Sciences; University of Macau; Taipa, Macao, P.R. China; Tel.: +853.397.4695; Fax: +853.841.358; Email: simonlee@umac.mo/Prof. Yi-Tao Wang; Institute of Chinese Medicine Sciences; University of Macau; Taipa, Macao, P.R. China; Tel.: +853.397.4691; Fax: +853.841.358; Email: ytwang@umac.mo

Original manuscript submitted: 12/13/06
Manuscript accepted: 04/20/07

Previously published online as a *Cancer Biology & Therapy* E-publication:
http://www.landesbioscience.com/journals/cbt/article/4317

KEY WORDS

furanodiene, apoptosis, $HepG_2$, caspase-3, mitochondrial, cytochrome c, p38, ERK

ACKNOWLEDGEMENTS

This study is supported by the grant from the Research Committee, University of Macau, Macao SAR (Ref. No. RG054/05-06S and RG058/05-06S) and grant from the Science and Technology Development Fund, Macao SAR (Ref. No. 012/2006/A).

ABSTRACT

Furanodiene ($C_{15}H_{20}O$), a pure compound isolated from Traditional Chinese medicine, *Curcuma wenyujin*, named Ezhu in Chinese, which structure was determined on the basis of NMR, MS and UV spectrum. In this study, we attempted to characterize in detail the signaling cascades resulted from furanodiene-induced apoptosis in human hepatoma HepG2 cells. Furanodiene inhibited HepG2 cell growth by causing cell cycle arrest at G_2/M and inducing apoptosis as evidenced by DNA fragmentation assay. We found that furanodiene induced mitochondrial transmembrane depolarization, release of mitochondrial cytochrome c, activation of caspases-3 and the cleavage of PARP. The furanodiene mediated mitochondria-caspase apoptotic pathway also involved activation of p38 and inhibition of ERK mitogen-activated protein kinase (MAPK) signaling. These results for the first time have identified the biological activity of furanodiene against HepG2 cells and provide rationales for further development of essential oil of Ezhu and its ingredients such as furanodiene on treatment of liver diseases.

©2007 LANDES BIOSCIENCE. DO NOT DISTRIBUTE.

INTRODUCTION

Curcuma belongs to the Family Zingiberaceae. This genus is composed of about 70 species of rhizomatous herbs which distributed all over the world. About 20 species could be identified in China, of which a few are traditional Chinese medicine being used for a long time. Chinese Pharmacopoeia indicated that the rhizomes of three species including *Curcuma phaeocaulis*, *C. kwangsiensis* and *C. wenyujin* are used as Chinese medicine and they are named as Ezhu in Chinese.[1] The essential oil of Ezhu has been reported to possess various biological roles such as, antimicrobial activity,[2] anti-inflammatory[3] and anti-tumor activity.[4,5] Furanodiene, a sesquiterpene compound, has been isolated from essential oil of *Curcuma wenyujin*.[6,7] Furanodiene hás been identified to have anti-inflammatory effects[8] and hepatoprotective effects.[9,10]

Many sesquiterpenes are identified to possess protective effects against carcinogenesis or tumour growth. Artemisinin (AR), a sesquiterpene lactones, killed human oral cancer cells through apoptosis and has been suggested that artemisinin may be useful as an alternative treatment for oral cancer.[11] Artemisinin has also demonstrated to have potent antiproliferative effects in vitro against P388 and A549 cells. This activity reflected in P388 murine leukemia by an accumulation of cells in G_1 phase, and induction of apoptosis[12] and displayed cytotoxicity to cloned murine Ehrlich ascites tumor (EAT) cells and human HeLa cells and against murine bone marrow using a clonogenic assay for committed progenitor cells of the granulocyte-monocyte lineage. Another compound, sesquiterpene lactones, Cynaropicrin from Saussurea lappa, has been reported to be a potential anticancer agent against some leukocyte cancer cells such as lymphoma or leukemia, through pro-apoptotic activity.[13] Glyceroglycolipids from Serratula strangulate also possess cytotoxicity to SMMC-7721, B16 and HeLa cells.[14]

Hepatocellular carcinoma is the fifth most commonly diagnosed cancer with more than 1 million deaths reported annually worldwide.[15] In order to develop effective means for prevention and treatment of hepatocellular carcinoma and related liver diseases. We have isolated and identified several chemical extracts and pure compounds from Chinese medicine with anti-hepatoma, anti-multidrug resistant hepatoma and anti-hepatitis viral effects.[16-19] Essential oil of Ezhu and it active ingredients have been widely used for treatment of malignant tumors in China.[4,5] Furanodiene, an ingredient from Ezhu oil, has been identified to have protective effects against D-galactosamine/

lipopolysaccharide/TNFα induced liver injury.[9,10] In order to control the consistence of chemical composition and efficacy of Ezhu for clinical use, we have quantitatively determined the chemical compositions of different species and cultivated sources of Ezhu in China.[6,7] In present study, we attempt to determine the cytotoxicity of furanodiene in human hepatoma HepG2 cells and its action of molecular mechanism.

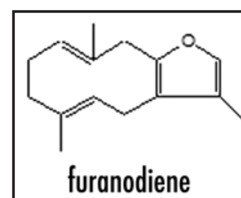

Figure 1. Chemical structure of furanodiene.

MATERIALS AND METHODS

Materials. Furanodiene ($C_{15}H_{20}O$) was isolated and purified at the Institute of Chinese Medical Sciences, University of Macau. (Macau, China) as described.[6,7] In brief, furanodiene was isolated and purified from Ezhu by silica-gel-column separation, medium pressure liquid chromatography (MPLC) and preparative HPLC (pre-HPLC). The purity of the compound was tested by HPLC-DAD. The structure, as shown in Figure 1 was confirmed by UV, MS and NMR analysis. Formula: $C_{15}H_{20}O$, MW: 216. EI-MS: 216(M+, 52), 201(19), 159(26), 148(6), 145(27), 108(100), 91(33), 77(27), 65(14), 53(16), 41(27).

MTT, JC-1 dye, caspase-3 Assay kit, and 488 Cytochrome c Apoptosis Detection Kit were purchased from Molecular Probes. Human Apoptosis Kit, Cell Signal Master Buffer Kit, Phospho p38 (T180/Y182) Flex Set, Phospho ERK1/2 (T202/Y204) Flex Set and Phospho JNK1/2 (T183/Y185) Flex Set were purchased from BD Bioscience.

Cell culture and drug treatment. Human hepatoma cell line HepG2 was obtained from the American Type Culture Collection (ATCC, Rockville, MD). Cells were cultured with RPMI 1640 medium (GIBCO, Grand Island, NY) supplemented with 10% (v/v) heat-inactivated fetal bovine serum (FBS) (Life Technologies Inc., Gaithersburg, MD), 100 μg/ml streptomycin and 100 unit/ml penicillin in 75 cm^2 tissue culture flasks at humidified incubator at 37°C with 5% CO_2. Furanodiene (22 mg) was dissolved in 1 ml DMSO to make a 1 mM stock solution and was then diluted to different concentrations as needed. The final volume of drug solution added to medium was 1%. Control samples contain 1% DMSO.

Growth inhibitory assay. Cells were seeded in 96-well microplates (1 x 10^5 cells/well in 100 μl medium). Furanodiene was added to the cells in serial concentrations and was incubated for 48 hours. Medium was discarded before 30 μl of tetrazolium dye (MTT) solution (5 mg/ml in PBS) was added to each well and incubated for additional four hours. DMSO (10 μl) was added to dissolve the formed formazan crystals. The plate was then read in a microplate reader at 570 nm. MTT solution with DMSO (without cells and medium) acted as blank while the DMSO (1%)-treated cells served as control of 100% survival.

Agarose gel electrophoresis for analysis of DNA fragmentation. HepG2 cells were treated with drug for 24–72 hours while the DMSO (1%) containing medium treated cells served as control. Adherent cells (2 x 10^6/ml) were harvested and washed once with 400 μl PBS. The washed-cells were fully suspended in 400 μl of lysis buffer (containing 200 mM Tris-HCl (pH 8.3), 100 mM EDTA and 1% SDS). Twenty microliters of 10 mg/ml proteinase K was added to digest the proteins, and then the tubes were incubated in a 37°C water bath overnight. The samples were allowed to cool down to room temperature and 300 μl of saturated NaCl solution was added. After centrifuging for 15 min at 9000 rpm, supernatants were collected. DNA fibers were obtained by adding 1 ml of cold absolute ethanol (EtOH) and centrifuged for 20 min at 4°C at 16,000 rpm. Then, DNA fibers were washed once with 500 μl of -20°C 70% EtOH and then DNA pellet was dried in a 70°C oven. After dried-DNA pellet was obtained, 15 μl of TE buffer (10 mM Tris-HCl pH 8.0, 1 mM EDTA) containing 0.2 mg/ml of RNase A was added, and incubated at 37°C for 90 min. 10 μl of each DNA samples were loaded on a 1.5% TBE agarose gel to observe the appearance of DNA ladder.

Cell cycle analysis. Cells were seeded at 6-well plates and treated with furanodiene at desired concentrations for 48 and 72 hours. DMSO (1%)-treated cells served as control. After treatment, mediums were discarded. The adherent cells were washed with PBS, and then 300 μl of trypsin was added to detach the cells for 5 min incubation at room temperature. After centrifuging at 350 g at 4°C for 5 min, the cell pellet was obtained. Then the cell pellet was resuspended with 1ml cold 70% EtOH at 4°C for 12 hours. The cell pellet was centrifuged again for 5 min at 4°C at 350 g. Finally, 1 ml propidium iodide (PI) staining solution (20 μg/ml PI, 8 μg/ml DNase free RNase) was added to the samples. The samples were analyzed by a flow cytometry (BD FACS Canto™). The results were analyzed by Mod Fit LT 3.0 software.

Measurement of alternation of mitochondrial transmembrane potential (ΔΨm). ΔΨm was assessed by JC-1 (5,5',6,6'-tetra-chloro-1,1',3,3'-tetraethylbenzimidazolylcarbocyanine iodide), Mitochondrial Potential Sensors (Molecular Probes, Leiden, Netherlands). Red fluorescence J-aggregate form of JC-1 indicates intact mitochondria, whereas green fluorescence shows monomeric form of JC-1 due to breakdown of the mitochondrial membrane potential. Cells were seeded in 6-well plates and then incubated with desired concentrations of furanodiene for 48 hours. The medium of each well was discarded and treated with 1 ml medium (5 mg/ml JC-1) for 15 min at 37°C and 5% CO_2 in the dark, then washed twice in PBS. The cells were collected and centrifuged, the cell pellet resuspended in 1 ml of medium and measured by a flow cytometry.

Immunostaining of Cytochrome C. Cytochrome C release was assessed by SelectFX Alexa Fluor 488 Cytochrome C Apoptosis Detection Kit (Molecular Probes, Leiden, Netherlands). Cells were seeded in 24-well plate, and treated with desired furanodiene concentrations for 24 hours in a humidified incubator (37°C in 5% CO_2) for 24 hours while the DMSO (1%)-treated cells served as control. The medium were discarded and the cells were washed with warm PBS, fixed with fresh 4% formaldehyde in PBS for 15 min at 37°C, and permeabilized with 0.2% Triton X-100 for 5 min at room temperature. The cells were washed and incubated in a blocking buffer [10% heat-inactivated normal goat serum (NGS)] for 30 min at room temperature. And then the cells were incubated for one hour with 1 μg/mL primary antibody (anti-cytochrome C, mouse IgG) at room temperature. Green fluorescence was observed by a fluorescent microscope.

Caspase-3 enzymatic activity assay. Caspase-3 enzymatic activity was determined by measuring the cleavage of Ac-DEVD-R110

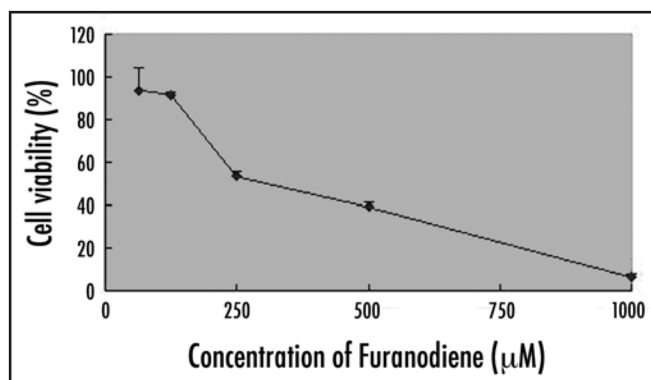

Figure 2. HepG2 was treated with different concentrations of furanodiene for 48 hours. Cell growth was determined by the MTT assay and was directly proportional to the absorbance at a wavelength of 570 nm. Data expressed as mean ± S.D. from three independent experiments.

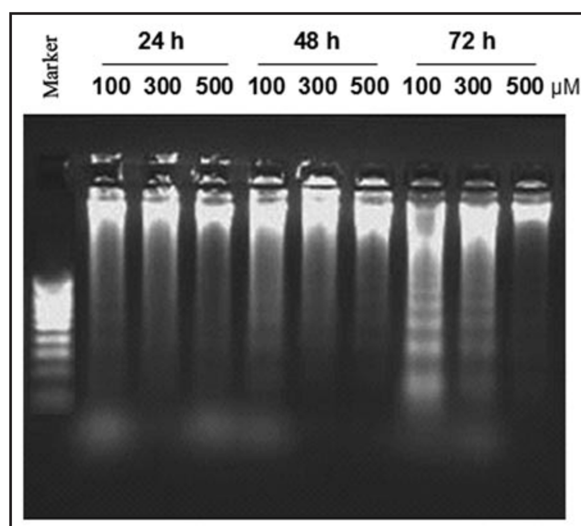

Figure 3. Agarose gel of electrophoresis of genomic DNA of HepG2 cells treated with different concentrations of furanodiene for 24–72 hours. DNA fragmentation with a ladder pattern is a characteristic of apoptosis.

according to the protocol with the caspase-3 assay kit supplied by Molecular Probes. Cells were treated with desired furanodiene concentrations in a humidified incubator (37°C in 5% CO_2) for 48 hours while the DMSO (1%)-treated cells served as control. Cells were harvested at a concentration of a minimum of 1 x 10^6 /ml, pellets were collected, appropriate cell lysis buffer was added and the samples were incubated on ice for 30 minutes. The samples were then centrifuged and supernatants were collected and transferred to microplate. Cell lysis buffer was used as a no-enzyme control to determine the background fluorescence of the substrate. At the same time, 1 μL of 1 mM Ac-DEVD-CHO inhibitor was added to selected samples. One microliter of DMSO was added to no-inhibitor samples to serve as control and incubated for ten minutes simultaneously. Then, 0.05 mM Z-DEVD-R110 substrate was added and incubated for 30 minutes prior to the fluorescence measurement.

Measurement of cleaved PARP and active caspase-3 protein levels. The BD™ CBA Human Apoptosis Kit (BD, Franklin Lakes, USA) was applied to quantify the active caspase-3 and PARP protein levels; Cytometric Bead Array (CBA) employs a particle with a discrete fluorescence intensity to detect a soluble analyte. This kit provided two types of bead populations with distinct fluorescence intensities that have been coated with capture antibodies specific for cleaved caspase-3 and PARP. Cells were seeded in 6-well plate and incubated with desired concentrations of furanodiene in a humidified incubator (37°C with 5% CO_2) for 48 hours. 1.0 x 10^6 cells per each sample were counted and harvested and then washed with PBS. Fifty microliters of cell lysis buffer was added to each sample for 30 min on ice and vortex at 10-minute intervals. Pellet cellular debris was removed by centrifugation at 12,500 rpm for ten minutes. Protein concentrations of all samples were measured by 2-D Quant Kit (Amersham Biosciences, Piscataway, USA). Each sample was normalized in a final concentration of 0.2 μg/μl. Thirteen standard curves (standard ranging from 0 to 6000 unit/ml) were obtained from one set of calibrators. For each sample and the standard mixture of lysate standard (caspase-3 and PARP beads), 50 ml of sample or standard of beads were added to the mixture of 50 ml of 2 mixed capture beads incubated for one hour, and then mixed 50 ml of PE detector bead for another one hour. After that, samples were washed before data acquisition with a flow cytometry. The results were analyzed by FCAP Array V1.0.

Measurement of expression levels of phospho-ERK1/2, phospho-JNK1/2 and phospho-p38. Expression of ERK1/2, JNK1/2 and p38 were measured by Cell Signaling Master Buffer Kit (BD, Franklin Lakes, USA). Three beads in a BD CBA provided a capture surface for specific proteins like phospho ERK1/2, phospho JNK1/2 and phospho p38 proteins. All procedures were carried out as described in above mentioned BD™ CBA Human Apoptosis Kit, except at which cell-denaturation buffer was used in stead of lysis buffer. Cell-denaturation buffer containing sample was placed in a boiling water bath for 5 min immediately. Pellet cellular debris were removed by centrifugation at 10,000 g for 5 min. Ten standard curves (standard ranging from 0 to 1000 pg/ml) were obtained from one set of calibrators. For each sample and the standard mixture of lysate standards (phospho ERK1/2, phospho JNK1/2 and phospho p38 beads), 50 ml of sample or standard of beads was added to the mixture of 50 ml of 3 mixed capture beads and 50 ml PE detector beads were incubated for four hours. After that, samples were washed before data acquisition with a flow cytometry. The results were analyzed by FCAP Array V1.0.

Statistical analysis. The data are expressed as mean ± S.D. from at least three independent experiments. Differences between groups were analyzed using a Student's t-tests.

RESULTS

Furanodiene inhibits cells growth and induces DNA fragmentation in HepG2 cells. Furanodiene treatment inhibited the growth of HepG2 cells in a dose-dependent manner, and the IC_{50} of furanodiene was approximately 300 μM (Fig. 2). We then examined whether furanodiene inhibited HepG cell growth through inducing cell death and apoptosis. HepG2 cell were treated with different concentrations of furanodiene for 24–72 hours. Figure 3 showed that DNA ladder and fragmentation was evidently observed, especially at the concentrations of 100 and 300 μM after 48 and 72 hours treatments.

Furanodiene causes G_2/M cell cycle arrest. The effect of different concentrations of furanodiene on cell-cycle progression was studied after 48 and 72 hours of drug exposure. Furanodiene treatment resulted in a dose- and time-dependent accumulation of cells in G_2/M phase with concomitant losses from G_0/G_1 phase (Fig. 4A and B).

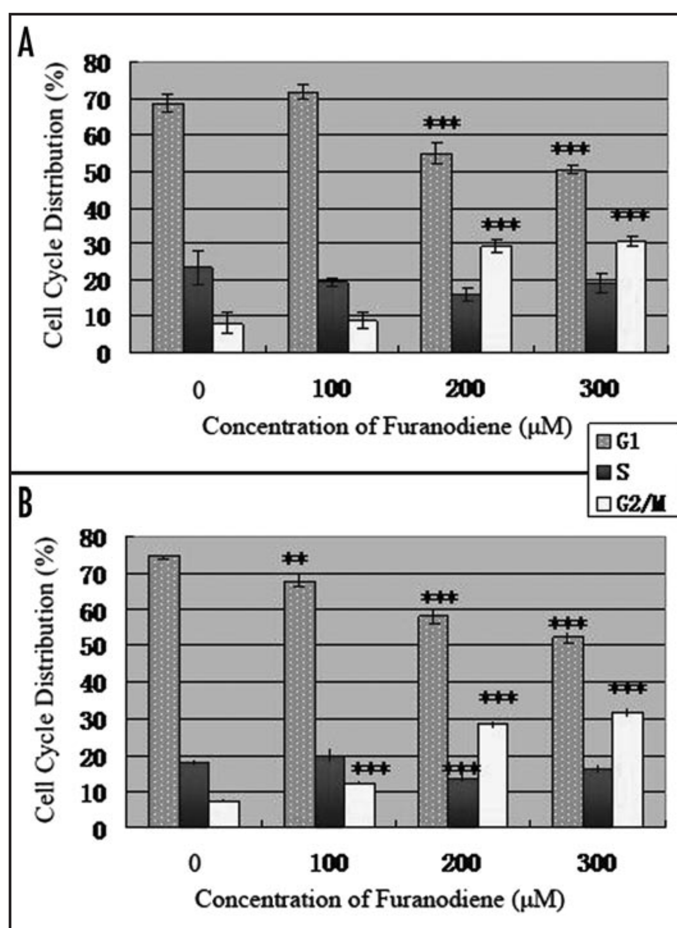

Figure 4. Effect of furanodiene in cell-cycle distribution of HepG2 cells. Flow cytometric analysis of propidium iodide-stained HepG2 cells treated with 100–300 μM furanodiene for 48 h (A) and 72 h (B). The results of HepG2 cells treated with furanodiene were analyzed by Mod Fit LT 3.0. Data expressed as mean ± S.D. from three independent experiments. $^{**}p < 0.01$; $^{***}p < 0.001$ versus control.

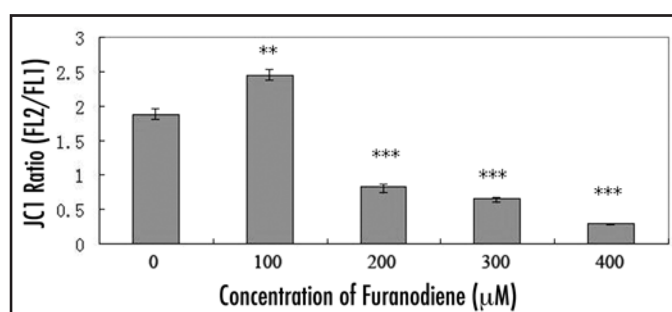

Figure 5. Analysis of change of mitochondrial transmembrane potential in HepG2 cells. HepG2 treated with 100, 300 and 500 μM furanodiene for 48 hours, were stained with JC-1 probe. The cells were analyzed by flow cytometry. Red Fluorescence and Green Fluorescence were measured by FL2 and FL1 channel respectively. Red fluorescence indicates intact mitochondrial potential while green fluorescence indicates breakdown of mitochondrial potential. The ratio of intensity of FL2 to FL1 indicates the change of mitochondrial transmembrane potential. Data expressed as mean ± S.D. from four independent experiments. $^{***}p < 0.001$ and $^{**}p < 0.01$ versus control.

The changes in cell cycle were much more dramatic when exposure time increased from 48 to 72 hours.

Furanodiene causes mitochondrial transmembrane depolarization in HepG2 cells. Some chemotherapeutic drugs induced apoptosis via mitochondrial pathways by altering mitochondrial transmembrane potential, $\Delta\Psi m$. To monitor the $\Delta\Psi m$, we used JC-1 probe to detect the $\Delta\Psi m$ after cells were treated with different concentrations of furanodiene for 48 hours. Mitochondria with normal $\Delta\Psi m$ concentrates JC-1 into aggregates (red/orange fluorescence), while in depolarized mitochondria, JC-1 forms monomers (green fluorescence). As compared to untreated HepG2 cells (control), the green fluorescence increased while the red/orange fluorescence decreased after exposure to furanodiene. Figure 5 indicated that little shift from red/orange to green fluorescence was observed in 100 μM furanodiene group while 200, 300 and 500 μM furanodiene groups, all showed a significant change in mitochondrial transmembrane potential.

Furanodiene causes cytochrome-c releasing from mitochondria into cytosol. Cytochrome c release from the mitochondria to the cytosol is implicated in mitochondria dependent apoptosis.[20] Cytochrome c staining in the cytosol of HepG2 cells showed markedly stronger green fluorescence than in control cells in a dose-dependent fashion (Fig. 6). Furanodiene treated cells showed obvious punctuate

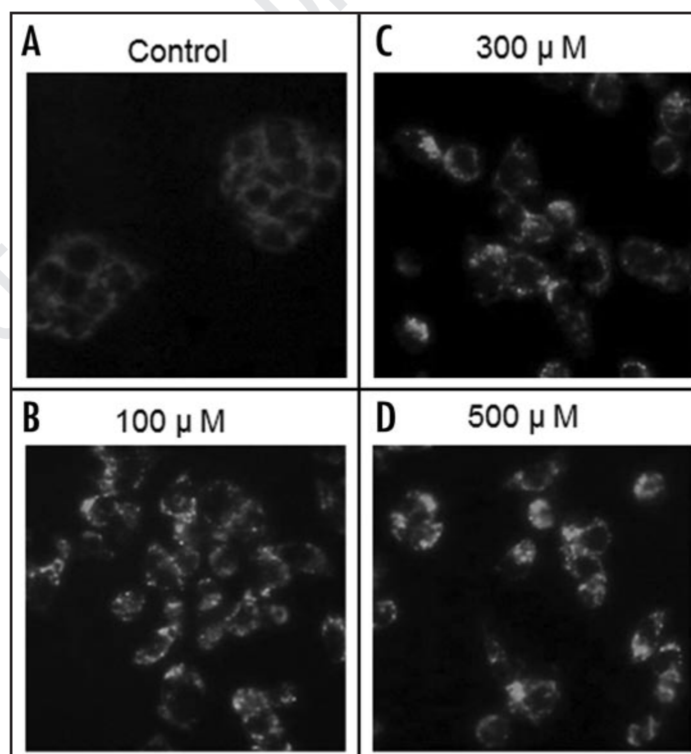

Figure 6. Cytochrome C release into the cytosol in furanodiene treated HepG2 cells. Cytochrome C immunofluorescence was observed with fluorescent microscope. (A) control; (B) 100 μM; (C) 300 μM; (D) 500 μM. Fine punctate/granular stainings for cytochrome c are observed. Cytochrome c release also increases the global cytosolic fluorescent signal. Similar results were obtained for three independent experiments. (Original magnification, 20×).

green fluorescence staining or appeared to have green fluorescence accumulated in large aggregates than in control cells.

Furanodiene activates caspase-3 enzymatic activity. Many studies previously have demonstrated that programmed cell death is associated with the activation of caspase as key elements involved in the sequence of events that lead to cell death.[21] Caspase-3 particularly,

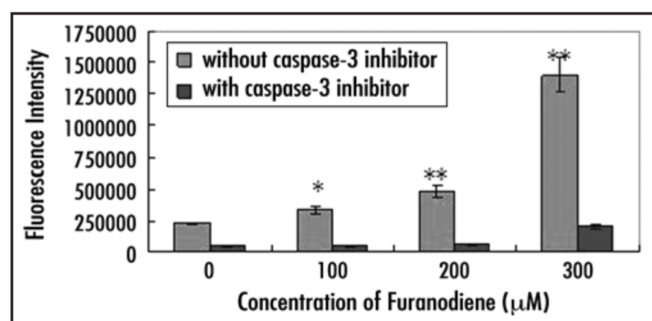

Figure 7. A concentration dependent increase in caspase-3 activation after 24 hours treatment with furanodiene. Caspase-3 cleaves substrate Ac-DEVD-R110 to emit green fluorescence. Higher fluorescent intensity indicates higher caspase-3 enzymatic activity. Ac-DEVE-CHO inhibitor can inhibit caspase-3 enzymatic activity. Data expressed as mean ± S.D. from three independent experiments. $^{**}p < 0.01$, $^{*}p < 0.1$ versus control.

is essential for propagation of the apoptotic signal after exposure to many DNA-damaging agents and anticancer drugs. Then, we examined caspase-3 activity after cells were treated with 100–300 μM furanodiene for 24 hours. The result clearly demonstrated that caspase-3 activity increased in a dose-dependent manner (Fig. 7). Caspase-3 activities were two and six times enhanced on 200 and 300 μM of furanodiene treatment groups respectively as compared to the control. When the cellular samples were incubated with specific Ac-DEVD-CHO inhibitors simultaneously, the caspase-3 activity was blocked.

Furanodiene increases cleaved PARP and active caspase-3 protein levels. Drug-induced cell death via apoptosis pathway, signaling can generally be divided into receptor- and mitochondrial-mediated pathways. These pathways converge at several downstream points including the mitochondria, caspase activation, and substrate cleavage.[22] Figure 8 showed that there was significant increase in protein levels of cleaved PARP and active caspase-3 in a does-dependent manner as determined by BD™ CBA (Cytometric Bead Array) Human Apoptosis Kit. HepG2 cells treated with 100, 200 and 300 μM of furanodiene were 3, 22 and 44 times higher in caspase-3 protein level than control group (Fig. 8A). The level of cleavage of PARP had 6-folds increase in HepG2 cells treated with 300 μM furanodiene compared to the control (Fig. 8B).

Furanodiene increases phospho-p38 and decreases phospho-ERK MAPK proteins levels. In order to evaluate if furanodiene induced the HepG2 cell death through activation of the cell signaling cascades of mitogen-activated protein kinases (MAPKs), we assessed the kinetics of p38 MAPK, ERK1/2 and JNK phosphorylation by BD™ CBA Cell Signaling Flex Set system. Figure 9 showed that the expression levels of phosphorylated p38 and phosphorylated ERK1/2 were regulated in opposite directions in furanodiene-induced HepG2 cell death at which phospho-p38 significantly increased in a dose dependent manner while phospho-ERK1/2 significantly diminished. Expression level of phospho-JNK was measured simultaneously with phospho-p38 and phospho-ERK1/2 but there was only a slight and statistically insignificant change in phospho-JNK level (Data not shown).

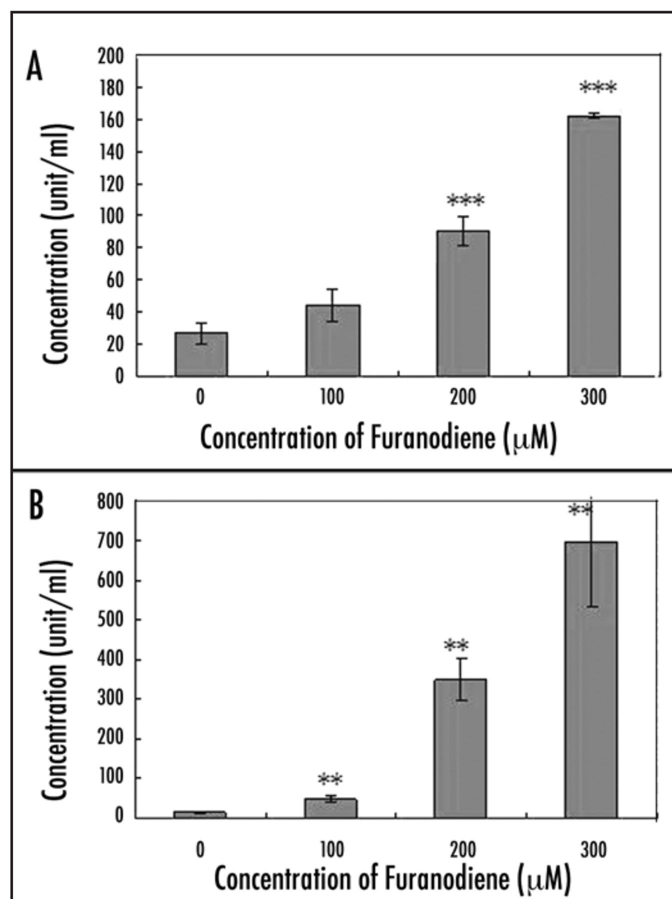

Figure 8. Protein expression levels of active caspase-3 and cleaved PARP in furanodiene-induced apoptosis. HepG2 cells were treated with medium alone (control) or different concentration of furanodiene for 48 h. Cells of each sample were counted to 1.0×10^6 and all the samples were normalized to final protein concentration in 0.2 μg/μl. It was detected with BD™ CBA Human Apoptosis Kit (BD, Franklin Lakes, USA) according to manufacturer instruction. The results were analyzed by FCAP Array V1.0. Active caspase-3 protein level in HepG2 was shown in (A) and the cleaved PARP protein level in HepG2 was shown in (B). The x-axis indicated the concentration of furanodiene while the y-axis indicated amount of proteins (unit per ml). Concentration of active caspase-3 and cleaved PARP in test samples were determined using the standard curve. Data expressed as mean ± S.D. from three independent experiments. $^{**}p < 0.01$; $^{***}p < 0.001$ versus control.

DISCUSSION

The essential oil of Ezhu and it's ingredients have been widely used for treatment of malignant tumors in China[5] and has been identified to have hepatoprotective effects.[9,10] In order to identify the active ingredients and mechanism of action of this herb, we have quantitatively determined the chemical compositions of different species and cultivated sources of Ezhu including *Curcuma phaeocaulis*, *C. kwangsiensis* and *C. wenyujin* in China.[6,7] We have found that the essential oil extract of *Curcuma wenyujin* inhibited HepG2 cells growth with IC50 at approximately 70 μg/ml (Data not shown). Thus, we are interested to further identify active ingredients in that herb. Furanodiene, a sesquiterpene compound, had been isolated from essential oil of *Curcuma wenyujin* previously and the furanodiene-induced apoptotic mechanism on HepG2 cells was studied. Apoptosis is a tightly regulated process under the control of several pathways, such as mitochondrial- and caspase-dependent pathways.[20,21] In present study, furanodiene has been identified to inhibit HepG2 cell growth via inducing apoptosis as evidenced by activation of depolarization of mitochondrial transmembrane

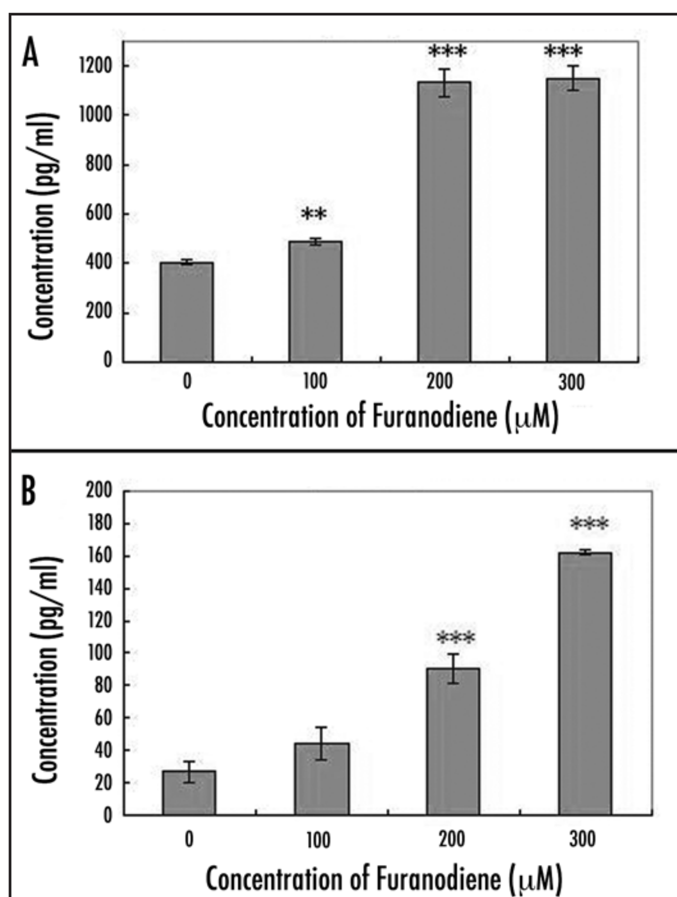

Figure 9. (A) phospho p38 expression level; (B) phospho ERK1/2 expression level. HepG2 cells were treated with medium alone (control) or different concentration of furanodiene for 48 h. Phosphorylation of p38 MAPK and ERK1/2 were determined by BD™ CBA Cell Signaling Flex Set system according to manufacturer instruction. Data expressed as mean ± S.D. from three independent experiments. **$p < 0.01$; ***$p < 0.001$ versus control.

potential, mitochondrial cytochrome-c release, caspase-3, PARP cleavage, G_2/M cell cycle arrest and finally DNA fragmentation.

In order to confirm the apoptosis was mediated by furanodiene, the uptake of furanodiene in HepG2 cells was quantitatively measured using HPLC method. When HepG2 cells were treated with 2 ml culture medium containing 300 μM furanodiene for six hours, the amount of furanodiene absorbed into 10^6 cells is 2.57 x 10^{-9} mol which is equivalent to 4.3% of total amount of furanodiene in culture medium (Data not shown).

Active caspase-3 has been considered to be indicative of apoptosis[21] and another characteristic event of apoptosis is the proteolytic cleavage of PARP, a nuclear enzyme involved in DNA repair, DNA stability, and transcriptional regulation.[23] Furanodiene induced significant increase in caspase-3 enzymatic activity as well as the protein levels of active caspase-3 and cleaved PARP (Figs. 7 and 8). These results suggested that furanodiene induced apoptosis via caspase pathway. Moreover, whether furanodiene induced apoptosis in HepG2 cell is mitochondria-dependent is unknown. To address this question, the change of mitochondrial transmembrane potential ($\Delta\Psi$m), and mitochondrial cytochrome c release were determined. Figures 5 and 6 suggested that the furanodiene-mediated apoptosis was accompanied with the $\Delta\Psi$m as well as the release of mitochondrial cytochrome c into cytosol. These results demonstrated that a mitochondrial pathway was also involved in furanodiene-induced apoptosis.

The mitogen-activated protein kinase (MAPK) superfamily consists of three serine/threonine kinase cascades.[24] Extracellular-signal-related kinases (ERKs) respond to growth factors or other external mitogenic signals by promoting cell proliferation and opposing cell death signals. The other two pathways—p38 MAPK and the c-Jun N-terminal kinase (JNK) pathways—are typically described as stress-activated kinases that promote programmed cell death.[25] It is now widely believed that p38 and JNK mediate apoptotic signals, while ERK promotes growth, differentiation, and proliferation. Nowadays, many studies have shown that p38 MAPK activation is necessary for cancer cell death initiated by a variety of anti-cancer agents.[26] Four chemotherapeutic agents have been shown to induce mitotic cell-cycle arrest through p38 activation in HeLa human cervical carcinoma cells and p38 MAPK activation is necessary for these chemotherapeutic drugs-induced cell death.[27]

Furthermore, different MAPK signaling pathways can be coordinately manipulated to enhance the efficacy of anticancer drug. Cotreatment of anticancer drugs with ERK inhibitors has been found to enhance anticancer effects. Anti-cancer drug paclitaxel (Taxol) induces tumor cell apoptosis through activating endogenous JNK in tumor cells.[28] When paclitaxel and ERK inhibitor were combined in cancer treatment, ERK inhibitor significantly enhances the JNK activation-mediated cytotoxic effect of paclitaxel.[28] ERK inhibitor also found to enhance docetaxel-induced apoptosis of androgen-independent human prostate cancer cells.[29]

In our experiments, as shown in Figure 9, furanodiene obviously elevated phosphorylated form of p38 and reduced phosphorylated form of ERK1/2 in a dose-dependent manner, but a slight and statistically insignificant change in phosphorylated form of JNK (data not shown). Therefore, furanodiene induced-apoptosis in HepG2, not only involve mitochondria-caspase pathways but also activation of P38 and inhibition of ERK MAPK signaling. It provides insight into the molecular action of furanodiene on HepG2 and provides clues for explanation of biological activities of furanodiene on treatment of liver diseases. The results are also important to provide rationales for further development of the Ezhu and its active ingredients on treatment of liver diseases and cancer. Although the cytotoxic effect of furanodiene to HepG2 cells is not as strong as those reported anticancer drugs, the chemical structure of furanodiene could be further modified to enhance its anti-tumour activities. Also, furanodiene could be used in combination with other chemotherapeutic drugs in order to allow the use of lower chemotherapeutic drug dosage, likely leading to lowered toxicity and enhanced tumor killing. In short, we conclude that furanodiene induces apoptosis in HepG2 cells through activation of mitochondrial and caspase-3-pathway which involved activation of P38, and inactivation of ERK1/2 MAPK signaling cascades.

References

1. Pharmacopoeia commission of PRC (editors), pharmacopoeia of the people's republic of china. Vol. I. Beijing, PR China: Chemical Industry Press, 2005:14-15.
2. Martins AP, Salgueriro L, Goncalves MJ. Essential oil composition and antimicrobial activity of three Zingiberaceae from S.Tome e Principe. Planta Med 2001; 67:580-4.
3. Tohda C, Nakayama N, Hatanaka F, Komatsu K. Comparison of anti-inflammatory activities of six Curcuma rhizomes: A possible curcuminoid-independent pathway mediated by curcuma phaeocaulis extract. Evid Based Complement Alternat Med 2006; 3:255-60.
4. Wan YW. Inhibitory effects of Curcuma aromatica oil on proliferation of hepatoma in mice. World J Gastroentero 2000; 6:216-9.
5. Peng X, Zhao Y, Liang X, Wu L, Cui S, Guo A, Wang W. Assessing the quality of RCTs on the effect of beta-elemene, one ingredient of a Chinese herb, against malignant tumors. Contemp Clin Trials 2006; 27:70-82.

6. Yang FQ, Li SP, Chen Y, Lao SC, Wang YT, Dong TT, Tsim KW. Identification and quantitation of eleven sesquiterpenes in three species of Curcuma rhizomes by pressurized liquid extraction and gas chromatography-mass spectrometry. J Pharm Biomed Anal 2005; 39:552-8.
7. Yang FQ, Li SP, Zhao J, Lao SC, Wang YT. Optimization of GC-MS conditions based on resolution and stability of analytes for simultaneous determination of nine sesquiterpenoids in three species of Curcuma rhizomes. J Pharm Biomed Anal 2007; 43:73-82.
8. Makabe H, Maru N, Kuwabara A, Kamo T, Hirota M. Anti-inflammatory sesquiterpenes from Curcuma zedoaria. Nat Prod Res 2006; 20:680-5.
9. Matsuda H, Ninomiya K, Morikawa T, Yoshikawa M. Inhibitory effect and action mechanism of sesquiterpenes from Zedoariae Rhizoma on D-galactosamine/lipopolysaccharide-induced liver injury. Bioorg Med Chem Lett 1998; 8:339-44.
10. Morikawa T, Matsuda H, Ninomiya K, Yoshikawa M. Medicinal foodstuffs. XXIX. Potent protective effects of sesquiterpenes and curcumin from Zedoariae Rhizoma on liver injury induced by *D-galactosamine/lipopolysaccharide* or tumor necrosis factor-alpha. Biol Pharm Bull 2002; 25:627-31.
11. Oda D, Habte T, Yamachika E. Artemisinin: An alternative treatment for oral cancer. Anticancer Res 2004; 204:2153-60.
12. Li Y. Novel antitumor artemisinin derivatives targeting G_1 phase of the cell cycle. Bioorg Med Chem Lett 2001; 11:5-8.
13. Jae YC, Ae RK. Cytotoxic and pro-apoptotic activities of cynaropicrin, a sesquiterpene lactone, on the viability of leukocyte cancer cell lines. European Journal of Pharmacology 2004; 492:85-94.
14. Jing QD, Qi XZ. Glyceroglycolipids from Serratula strangulate. Phytochemistry 2001; 58:1305-9.
15. Jemal A, Murray T, Ward E, et al. Cancer statistics, 2005. CA Cancer J Clin 2005; 55:10-30.
16. Tang PM, Chan JY, Au SW, Kong SK, Tsui SK, Waye MM, Mak TC, Fong WP, Fung KP. Pheophorbide a, an active compound isolated from scutellaria barbata, possesses photodynamic activities by inducing apoptosis in human hepatocellular carcinoma. Cancer Biol Ther 2006; 5:1111-6.
17. Lee SM, Li ML, Tse YC, Leung SC, Lee MM, Tsui SK, Fung KP, Lee CY, Waye MM. Paeoniae radix, a Chinese herbal extract, inhibit hepatoma cells growth by inducing apoptosis in a p53 independent pathway. Life Sci 2002; 71:2267-77.
18. Chan JY, Siu KP, Fung KP. Effect of arsenic trioxide on multidrug resistant hepatocellular carcinoma cells. Cancer Lett 2006; 236:250-8.
19. Lam WY, Leung KT, Law PT, Lee SM, Chan HL, Fung KP, Ooi VE, Waye MM. Antiviral effect of phyllanthus nanus ethanolic extract against hepatitis B virus (HBV) by expression microarray analysis. J Cell Biochem 2006; 97:795-812.
20. Brenner C, Kroemer G. Apoptosis: Mitochondria-the death signal integrators. Science 2000; 289:1159-64.
21. Thomberry AN, Lazebnik Y. Caspase: Enemies within. Science 1998; 281:1312-6.
22. Ferri KF, Kroemer G. Organelle-specific initiation of cell death pathways. Nat Cell Biol 2001; 3:E255-63.
23. Amours DD, Desnoyers S, Silva ID, Poirier GG. Poly(ADP)-ribosylation reactions in the regulation of nuclear functions. Biochem J 1999; 342:249-68.
24. Chang L, Karin M. Mammalian MAP kinase signaling cascades. Nature 2001; 410:37-40.
25. Xia Z, Dickens M, Raingeaud J, Davis RJ, Greenberg ME. Opposing effects of ERK and JNK-p38 MAP kinases on apoptosis. Science 1995; 270:1326-31.
26. Olson JM, Hallahan AR. P38 MAP kinase: A convergence point in cancer therapy. TRENDS in Molecular Medicine 2004; 10:125-9.
27. Deacon K, Mistry P, Chernoff J, Blank JL, Patel R. P38 mitogen-activated protein kinase mediates cell death and p21-activated kinase mediates cell survival during chemotherapeutic drug-induced mitotic arrest. Mol Biol Cell 2003; 14:2071-87.
28. MacKeigan JP, Collins TS, Ting JP. MEK inhibition enhances paclitaxelinduced tumor apoptosis. J Biol Chem 2000; 275:38953-6.
29. Zelivianski S, Spellman M, Kellerman M, Kakitelashvilli V, Zhou XW, Lugo E, Lee MS, Taylor R, Davis TL, Hauke R, Lin MF. ERK inhibitor PD98059 enhances docetaxel-induced apoptosis of androgen independent human prostate cancer cells. Int J Cancer 2003; 107:478-85.